

Supplemental Materials:

S1. Sample preparation and measurement method

Pt(10)/YIG(40, 60, 80, 100)/Pt(10) (thickness in nanometer) were prepared on the Si-SiO₂ substrates by an ultrahigh vacuum magnetron sputtering system (ULVAC, MPS-4000) at room temperature, and the base pressure is 3×10^{-6} Pa. After deposition, the 800 °C annealing in air for 1 h was carried out to improve the quality of the crystal structure of YIG [S1, S2]. Films were patterned into the structure as shown in Fig. 1(a) by photolithography combined with Ar ion etching, and the size of the strip is $120 \mu\text{m} \times 1000 \mu\text{m}$.

There are some differences for the preparation process of reference samples, because Cu is easy to be oxidized in air. Firstly, the Pt(10)/YIG(60) bilayer was deposited on a Si-SiO₂ substrate, then the 800 °C annealing in air for 1 h was done. After annealing, the Cu(10)/MgO(2) was deposited on the Si-SiO₂/Pt(10)/YIG(60). Then the Si-SiO₂/Pt/YIG/Cu/MgO film was patterned into two types of samples: when Pt is made for the injecting (bottom) electrode and Cu is made for the detecting (top) electrode, while the bottom and top electrodes are defined as injecting (applying current) and detecting electrodes (measuring voltage) in Fig. 1(a), we call it Pt/YIG/Cu; when Cu is made for the injecting (bottom) electrode and Pt is made for the detecting (top) electrode, we call it Cu/YIG/Pt.

A vibrating sample magnetometer (VSM, MicroSense, EZ-9) was used to measure the magnetic properties of these samples. The transport properties were measured in a physical property measurement system (Quantum Design, PPMS-9T), and the ferromagnetic resonance (FMR) absorption spectrum was measured on an electronic spin resonance spectrometer (JEOL, JES-FA200).

S2. HAADF result and FMR absorption spectrum

The high angle annular dark field (HAADF) image of the Pt(10)/YIG(100)/Pt(10) (thickness in nanometer) multilayer is shown in Fig. S1(a). The brightness is proportional to Z^2 , while Z is the atomic number. There is no element diffusion in this structure, and the interface between Pt and YIG is very clear and sharp. We also measured the ferromagnetic resonance (FMR) absorption spectrum in both Si-SiO₂/Pt(10)/YIG(60)/Pt(10) and GGG/YIG(60) samples at an rf power of 1 mW in an in-plane field, as seen in Fig. S1(b), and the amplification factor of the intensity is 1200 for Si-SiO₂/Pt(10)/YIG(60)/Pt(10) and 1.4 for GGG/YIG(60) respectively. Moreover, these two samples were prepared by the same process.

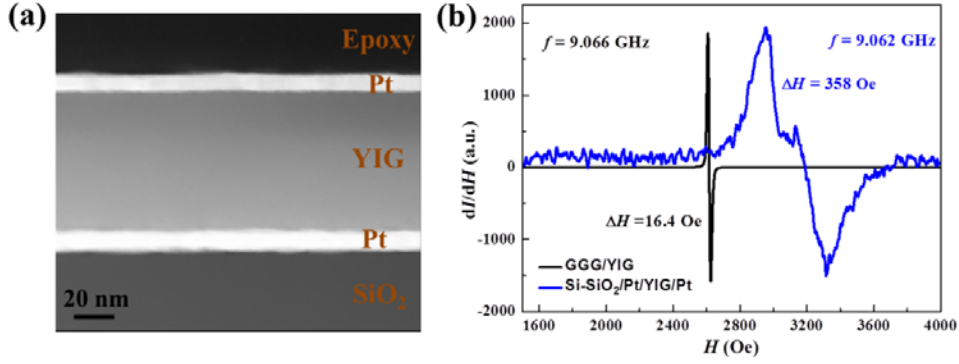


Fig. S1 (a) The high angle annular dark field (HAADF) image of the Pt(10)/YIG(100)/Pt(10) (thickness in nanometer) multilayer. (b) The ferromagnetic resonance (FMR) absorption spectrum measured in Si-SiO₂/Pt/YIG/Pt (blue line) and GGG/YIG (black line) samples. Resonance frequency and linewidth are given in the figure.

S3. Temperature dependence of electrical drag coefficient

By fitting the temperature dependent V_t - I_b curves with the formula $V_t/R_t = aI_b + bI_b^2$, we can obtain the temperature dependence of the electrical drag coefficient a , as shown in Fig. S2. Clearly, the data cannot be fitted with a simple power law. Instead, we have chosen to fit the a - T curve with the formula of $a = A(T-T_B)^{5/2} + B$, and a threshold temperature $T_B = 270$ K was obtained.

At present, the simple theory [S3, S4] was able to account for such relation. The threshold temperature indicates a gap in magnon spectra. However, the magnon gap for the soft ferromagnetic YIG is expected much smaller than T_B .

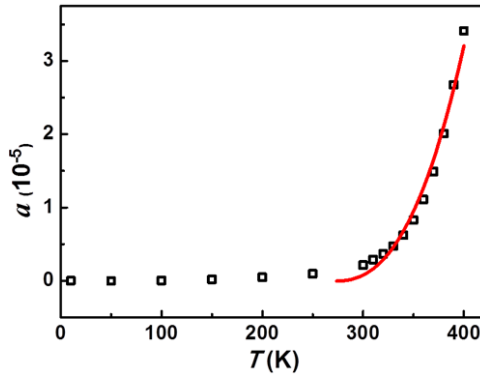


Fig. S2 The temperature dependence of the electrical drag coefficient a and the fitting curve by using $a = A(T-T_B)^{5/2} + B$ in the Pt/YIG/Pt sample.

S4. Magnetic field dependence of magnon drag voltage in x and z directions

The magnetic field dependence of the voltage in Pt/YIG/Pt with the magnetic field along x and z axis was measured, as shown in Fig. S3. As the voltage signal is proportional to the square of the y -component of the magnetization [S3, S4], it decreases with the increase of the magnetic field along x or z axis. At the coercive field where the magnetization along the x or z axis is zero, while the y -component is usually finite, so there is a considerable signal.

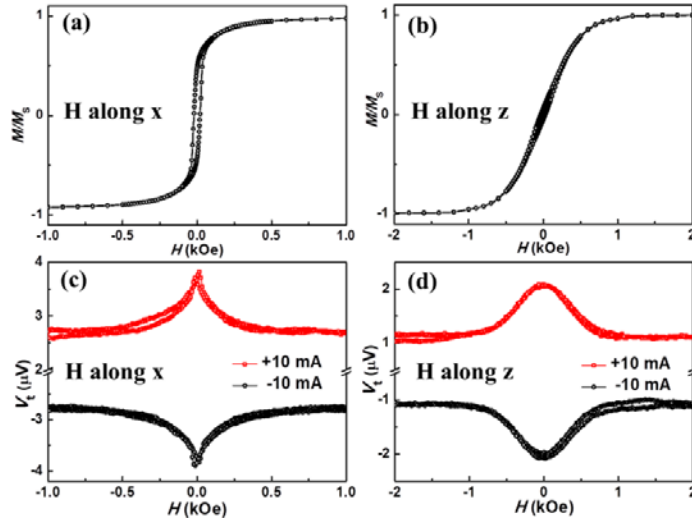


Fig. S3 (a) and (b) show the M - H loops with field along x and z axis respectively. The magnetic field dependence of the magnon drag voltage measured in the Pt/YIG/Pt sample, the magnetic field is scanned along x axis in (c) and z axis in (d).

S5. SMR in top and bottom Pt

The spin Hall magnetoresistance (SMR) in the bilayer YIG/Pt structure refers to the similar m_y^2 angular dependence of the resistance, due to the fact that the spin current whose spin polarization perpendicular to the magnetization of the YIG is absorbed at the interface [S5, S6]. We used the two-terminal method to measure the SMR for the bottom Pt/YIG interface or the top YIG/Pt interface alone. The R - H curves were measured with magnetic field along x , y and z axis, as shown in Fig. S4. The magnetization direction dependence of the SMR was also measured, as shown in Fig. S5. These results distinguish the SMR from the AMR.

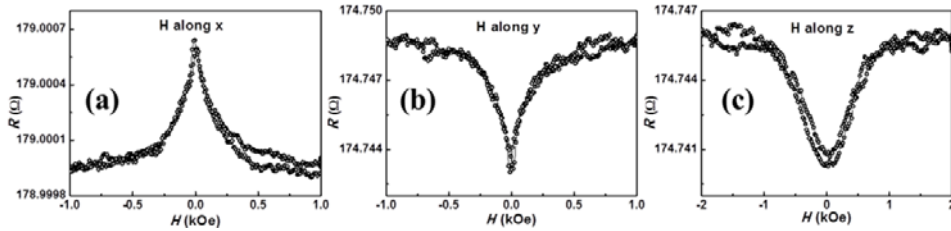


Fig. S4 The SMR measured in top (bottom) Pt in the Pt/YIG/Pt sample. (a), (b) and (c) show the R - H curves with field scanned along x , y and z axis respectively.

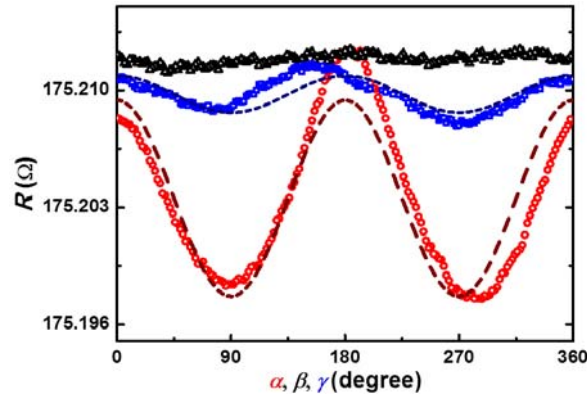


Fig. S5 The magnetization direction dependence of the SMR measured in the top (bottom) Pt layer in the Pt/YIG/Pt sample, a 3 kOe is applied to saturate the M of YIG in every direction while the sample is rotating. The angular α, β and γ are defined the same with that in the paper.

S6. Leakage current test

Finally, we checked the leakage current in the Pt/YIG/Pt sample, as shown in Fig. S6. The charge current was applied between the top Pt and the bottom Pt directly and the voltage was also measured between the top Pt and the bottom Pt. We have calculated the resistance between top Pt and bottom Pt to be larger than 14 M Ω .

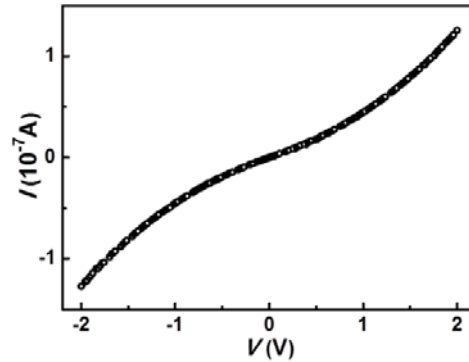


Fig. S6 The leakage current test measured in the Pt/YIG/Pt sample, the charge current and voltage are measured between the top Pt and bottom Pt layers.

References:

- S1. Y. M. Kang, S. H. Wee, S. I. Baik, S. G. Min, S. C. Yu, S. H. Moon, Y. W. Kim, and S. I. Yoo, *J. Appl. Phys.* **97**, 10A319 (2005).
- S2. X. T. Zhou, W. J. Cheng, F. T. Lin, X. M. Ma, and W. Z. Shi, *Appl. Surf. Sci.* **253**, 2108-2112 (2006).
- S3. Steven S. -L. Zhang and S. Zhang, *Phys. Rev. Lett.* **109**, 096603 (2012).
- S4. Steven S. -L. Zhang and S. Zhang, *Phys. Rev. B.* **86**, 214424 (2012).
- S5. S. Y. Huang, X. Fan, D. Qu, Y. P. Chen, W. G. Wang, J. Wu, T. Y. Chen, J. Q. Xiao, and C. L. Chien, *Phys. Rev. Lett.* **109**, 107204 (2012).
- S6. H. Nakayama, M. Althammer, Y. T. Chen, K. Uchida, Y. Kajiwara, D. Kikuchi, T. Ohtani, S. Geprags, M. Opel, S. Takahashi, R. Gross, G. E. W. Bauer, S. T. B. Goennenwein, and E. Saitoh, *Phys. Rev. Lett.* **110**, 206601 (2013).